AGU PUBLICATIONS

Geophysical Research Letters

RESEARCH LETTER
10.1002/2014GL061639

Key Points:
- A new high-resolution record of western tropical Pacific SST is presented
- Pleistocene pCO_2 was not the sole driver of tropical Pacific SST
- Tropical Pacific SST gradients may have influenced MPT climate

Supporting Information:
- Readme
- Table S1

Correspondence to:
K. A. Dyez,
kdyez@ldeo.columbia.edu

Citation:
Dyez, K. A., and A. C. Ravelo (2014), Dynamical changes in the tropical Pacific warm pool and zonal SST gradient during the Pleistocene, *Geophys. Res. Lett.*, *41*, 7626–7633, doi:10.1002/2014GL061639.

Received 3 SEP 2014
Accepted 22 OCT 2014
Accepted article online 24 OCT 2014
Published online 11 NOV 2014

Dynamical changes in the tropical Pacific warm pool and zonal SST gradient during the Pleistocene

Kelsey A. Dyez[1,2] and A. Christina Ravelo[3]

[1]Earth and Planetary Sciences, University of California Santa Cruz, Santa Cruz, California, USA, [2]Now at Lamont-Doherty Earth Observatory, Columbia University, Palisades, New York, USA, [3]Ocean Sciences, University of California Santa Cruz, Santa Cruz, California, USA

Abstract In the late Pleistocene, the atmospheric carbon dioxide concentration (pCO_2) is thought to be a primary driving force for tropical sea surface temperature (SST) change because glacial-interglacial changes in tropical Pacific SST covary with pCO_2. However, if the regional radiative effects of pCO_2 were the only agent of change, tropical SST gradients should have remained similar as pCO_2 varied with time. Instead, a new record of SST from the west Pacific shows that tropical SST gradients were different, even reversed, in the past, suggesting an important role for dynamical circulation changes. Specifically, changes in the temperature of upwelled source water, in addition to local pCO_2 forcing, influenced tropical Pacific SST. These dynamical changes, rather than pCO_2, may have shifted the background state of the tropics and even helped set the stage for the mid-Pleistocene transition.

1. Introduction

The heat content of the tropical Pacific affects global atmospheric and oceanic convection and climate patterns [*Cane*, 1998]. Previous work argued that tropical Pacific sea surface temperature (SST) was controlled by radiative forcing from atmospheric carbon dioxide concentrations (pCO_2) [*Lea*, 2004; *Medina-Elizalde and Lea*, 2005; *Lea et al*., 2006; *Herbert et al*., 2010]. An examination of SST gradients between locations can test such a "top-down" forcing mechanism; changes in gradients would imply that additional dynamical mechanisms also affect SST.

Some studies argue that changes in equatorial upwelling patterns and atmospheric and oceanic convection [e.g., *Lea et al*., 2000; *Koutavas et al*., 2002; *Koutavas and Lynch-Stieglitz*, 2005] indicate that local dynamics affect SST in the east Pacific. Here we focus for the first time on tropical SST gradients within the western Pacific warm pool. Today the warm pool is warmest in the center equatorial region and cools toward its off equatorial margins (Figure 1). While several studies suggest that the warm pool expands with increased global temperature [*Sun*, 2003; *Liu et al*., 2005; *Brierley et al*., 2009], others argue that it is stabilized by negative feedbacks, e.g., atmospheric evaporative cooling [e.g., *Knutson and Manabe*, 1995], high-altitude tropical clouds [e.g., *Ramanathan and Collins*, 1991], and/or atmospheric heat transport away from the tropics [e.g., *Wallace*, 1992]. Yet a third possibility for the west Pacific SST pattern is an inverted equator-to-margin SST gradient, similar to the modern eastern Pacific cold tongue (cooler water along the equator), which could arise from enhanced equatorial upwelling, thermocline depth changes, or cooler source water for equatorial upwelling. We present a new high-resolution record from the margin of the modern western Pacific warm pool (Figure 1) and suggest that the on- to off-equator SST gradient was reversed at times over the past 1.4 Ma, consistent with dynamical oceanographic changes in the west Pacific.

Additionally, the new record allows for a reassessment of previously published work [*Medina-Elizalde and Lea*, 2005] on the evolution of the zonal (west-east) SST gradient across the mid-Pleistocene transition (MPT), which marks a major shift from dominantly 40 kyr to dominantly 100 kyr climate cycles. We show that the zonal SST gradient, which has been used to estimate past atmospheric Walker circulation strength [*Koutavas et al*., 2002; *Wara et al*., 2005; *Dekens et al*., 2007], increased in both the glacials and during the MPT; this evidence suggests that the MPT involved dynamical circulation changes, rather than simply a response to "top-down" pCO_2 local forcing.

2. Materials and Methods

Mg/Ca measurements of the surface-dwelling planktic foraminifera *Globigerinoides ruber* (Figure 2a) were made at Ocean Drilling Program (ODP) Site 871 (5°33′N, 172°21′E, water depth 1255 m, sedimentation

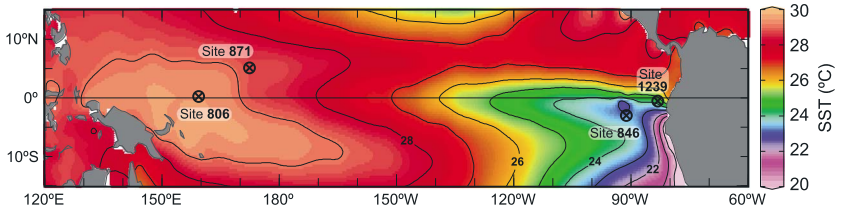

Figure 1. Selected tropical Pacific SST record locations and average annual surface temperature [*Locarnini et al.*, 2013] plotted using ODV [*Schlitzer*, 2014].

~1.0 cm/kyr [*Shipboard Scientific Party*, 1993]). The record has a resolution of one sample every ~3 kyr and combines previously published data for the past 0.5 Ma [*Dyez and Ravelo*, 2013] with new data covering 0.5 to 1.41 Ma. For each sample, 40–60 *G. ruber* (white) tests were picked from the 250–355 μm size fraction and cleaned following established protocols [*Boyle and Keigwin*, 1985; *Mashiotta et al.*, 1999]. Mg/Ca ratios were measured via inductively coupled plasma optical emission spectrometry at the University of California Santa Cruz (UCSC); 1σ standard deviation for repeated measurements of internal foraminifer reference standards is 0.21 mmol/mol, or ~0.5 °C.

To convert *G. ruber* Mg/Ca values to SST, we use an equation derived from nearby core top samples; $SST = \ln[(Mg/Ca_{measured} + 0.259 \times Depth\ (km) + 0.537)/0.38]/0.09$ [*Dyez and Ravelo*, 2013]. The same approach is applied to Site 806 published Mg/Ca values [*Medina-Elizalde and Lea*, 2005] to recalculate SST and

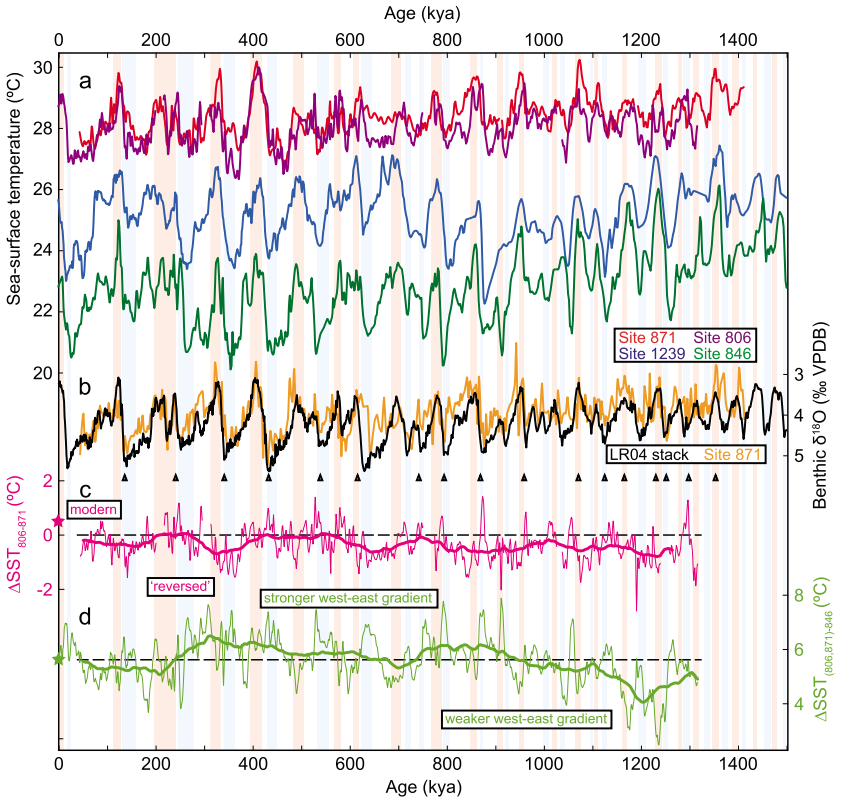

Figure 2. Equatorial Pacific SST records and gradients. (a) SST of ODP Sites 871 (44–500 kya [*Dyez and Ravelo*, 2013]; 500–1412 kyr, this study), 806 [*Medina-Elizalde and Lea*, 2005], 846 [*Liu and Herbert*, 2004], and 1239 [*Etourneau et al.*, 2010]. (b) Site 871 benthic $\delta^{18}O$ values aligned to a global benthic $\delta^{18}O$ stack [*Lisiecki and Raymo*, 2005]. (c) West Pacific equatorial gradient ($\Delta SST_{806-871}$); modern difference at star, breaks due to coring gaps at Site 806B [*Medina-Elizalde and Lea*, 2005]. (d) West-East Pacific gradient ($\Delta SST_{(806,871)\ -\ 846}$); modern value at star and dashed line. Vertical bars represent peak glacial and interglacial intervals.

thereby construct internally consistent regional temperature gradients. The resulting SSTs are ~0.3°C warmer than reported by *Medina-Elizalde and Lea* [2005].

For age model control of Site 871 (Figure 2b), we extended the benthic δ^{18}O record for Site 871 [*Dyez and Ravelo*, 2013] from 0.5 to 1.41 Ma. *Uvigerina* spp. tests (1–3 per sample) were ultrasonically cleaned, rinsed in methanol, and analyzed at UCSC using a Fisons PRISM mass spectrometer; precision based on replicate analyses of an internal Carrera marble reference standard was 0.05‰ (1σ). Benthic δ^{18}O stratigraphy was aligned with the LR04 benthic δ^{18}O stack [*Lisiecki and Raymo*, 2005] using time series matching software [*Palliard et al.*, 1996]. Glacial-interglacial amplitude of the Site 871 benthic δ^{18}O record is ~2.0‰ from 0 to 0.8 Ma and ~1.5‰ from 0.8 to 1.41 Ma, identical (within uncertainty) to the LR04 stack. The age model for Site 806 is also updated here by aligning benthic δ^{18}O [*Bickert et al.*, 1993; *Karas et al.*, 2009] with the LR04 benthic stack to improve temporal constraints on the SST gradient between Sites 871 and 806.

Peak glacial and interglacial intervals are defined for this study by selecting and averaging the portions of the LR04 stack that exceed a moving window of 1σ standard deviation (Table S1 in the supporting information). The window used is 40 kyr in the period 1.5–0.8 Ma and 100 kyr in the period 0.8–0 Ma, the approximate duration of glacial-interglacial cycles in each period. The same approach was used to select peak glacial-interglacial SSTs using the SST record. Although SST cycles lead benthic δ^{18}O cycles at the 100 kyr period by up to 12 kyr, whether we use the SST or the benthic δ^{18}O record to identify glacial and interglacial period does not impact our final results.

3. Results and Discussion

3.1. Site 871 SST Periodicity

The new Site 871 records are broadly similar to other tropical SST [*Liu and Herbert*, 2004; *Medina-Elizalde and Lea*, 2005; *Etourneau et al.*, 2010] and benthic δ^{18}O records [*Lisiecki and Raymo*, 2005] (Figures 2a and 2b). Spectral power in the SST record is greatest in the 41 kyr band prior to the MPT, in the 100 kyr band after the MPT, and is in phase with pCO_2 variability in the interval from which ice core pCO_2 records [*Jouzel et al.*, 2007] are available. This result suggests that on orbital timescales, radiative heating due to the regional direct and indirect effects of greenhouse gases is one of the drivers of open-ocean SST across the tropical Pacific [*Lea*, 2004; *Herbert et al.*, 2010; *Dyez and Ravelo*, 2013]. However, comparison of the off-equator Site 871 SST record to nearby equatorial Site 806 reveals that, superimposed on the pCO_2-driven SST changes, dynamical changes also play a role.

3.2. Western Pacific Upwelling

Modern SST at equatorial Site 806 is +0.4°C warmer than at off-equator Site 871. However, this difference ($\Delta SST_{806-871}$) over the past 1.4 Ma was highly variable and on average, reversed (-0.4 ± 0.6°C), suggesting that upwelling impacted equatorial SSTs in the past, even in the warm pool where the thermocline and mixed layer are deep. $\Delta SST_{806-871}$ is more pronounced prior to 800 ka (-0.5 ± 0.5°C), compared to afterward (-0.3 ± 0.5°C) (Figure 2c). Before further interpretation of the paleoceanographic conditions that might explain intermittent equatorial cooling, it is important to assess whether differential dissolution of foraminifer shells, which leads to lower Mg/Ca values and apparent cooling, impact the spatial or temporal variations in reconstructed SSTs.

Accurate reconstruction of $\Delta SST_{806-871}$ depends upon reliable SST estimates at each location. Estimates of Mg/Ca-based SST account for dissolution, which lowers the Mg/Ca of foraminifer shells at the seabed. Thus, the depth-dependent calibration we use [*Dyez and Ravelo*, 2013] takes into account the fact that Site 806 is ~1000 m deeper than Site 871 and results in an average $\Delta SST_{806-871}$ of −0.4°C. However, the original Site 806 data set [*Lea et al.*, 2000; *Medina-Elizalde and Lea*, 2005] did not account for dissolution; using the original method for both sites results in an average $\Delta SST_{806-871}$ of −1.5°C, a result that demonstrates the importance of correcting for dissolution. Although we apply a calibration [*Dyez and Ravelo*, 2013] that corrects for present-day differential dissolution, it does not account for past dissolution changes. As a first step, we must assess whether past dissolution changes could explain apparent changes in past $\Delta SST_{806-871}$.

Reconstructions of past changes in $\Delta[CO_3^{2-}]$ (saturation) isopleths [*Farrell and Prell*, 1989, 1991] show two important features with implications for our interpretation of $\Delta SST_{806-871}$. First, $\Delta[CO_3^{2-}]$ has been

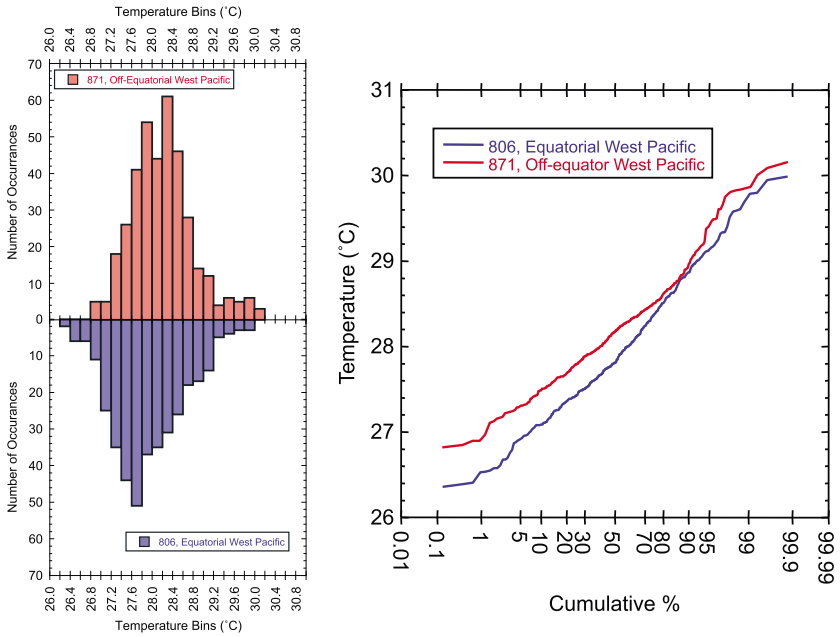

Figure 3. Probability density distribution of SST at off-equatorial Site 871 compared to equatorial Site 806. The two records were resampled at 2 kyr resolution and the distributions of each, displayed as (left) histograms and (right) cumulative %, show that the Site 806 distribution includes a larger proportion of cool SSTs relative to the Site 871 distribution.

increasing over the last 4 Myr such that prior to the MPT, deep waters were more corrosive, and likely caused more dissolution in the deep ocean than after the MPT [*Farrell and Prell*, 1991]. Because *Farrell and Prell* [1991] used sites deeper than 4000 m, it is difficult to assess whether changes in deep ocean chemistry also affected Site 806 (water depth 2520 m) and/or Site 871 (water depth 1250 m); but in a qualitative sense, the gradual increase in $\Delta SST_{806-871}$ through the MPT could be an artifact of gradually changing preservation affecting Site 806 slightly more than the shallower Site 871. Thus, without more information, we attribute the long-term change in $\Delta SST_{806-871}$ from an average value of ~ −0.5°C before the MPT to ~ −0.3°C after the MPT to changes in dissolution rather than in surface ocean conditions. Because Site 871 differs from Site 806 by being shallower and by having an off-equator location, it is unlikely to be affected by changes in dissolution or equatorial upwelling, and therefore provides a high-fidelity paleoceanographic record of western warm pool SST.

Second, although changing dissolution may explain the small change in average $\Delta SST_{806-871}$ at the MPT, the large glacial-interglacial variations in $\Delta[CO_3^{2-}]$ and dissolution [*Farrell and Prell*, 1989] cannot explain the observed $\Delta SST_{806-871}$ variations on orbital timescales. If deeper $\Delta[CO_3^{2-}]$ isopleths during glacials [*Farrell and Prell*, 1989] caused better preservation at both Sites 806 and 871, or only at deeper Site 806, it should have resulted in lower $\Delta SST_{806-871}$ values; in contrast, we find that $\Delta SST_{806-871}$ is generally greater during glacials (Figure 2c). Thus, if anything, deep ocean chemistry changes may be masking even larger changes in $\Delta SST_{806-871}$ than observed. Furthermore, spectral analyses of a percent-$CaCO_3$ record from a site near the modern lysocline (Site RC11-210, water depth 4420 m [*Thompson and Saito*, 1974; *Chuey et al*., 1987]) suggest that variability in $\Delta[CO_3^{2-}]$ occurred primarily at the 100 kyr periodicity, with no variability concentrated at the other orbital periods of 41 kyr and 23 kyr. Thus, the $\Delta SST_{806-871}$ variations at 41 kyr and 23 kyr, discussed later, cannot be an artifact of changes in dissolution.

Focusing on the last 800 kyr, after the MPT, both Site 871 and Site 806 (Figure 3) have similar maxima SSTs, but minima SSTs are cooler at equatorial Site 806 than at off-equatorial Site 871. If the effects of pCO_2 radiative forcing were solely responsible for changes in western warm pool temperature, both sites would be expected to have similar SST distributions in the past; the fact that their distributions are slightly different suggests that a secondary process modified western tropical Pacific SSTs. Cross-spectral analysis of $\Delta SST_{806-871}$ and pCO_2 [*Lüthi et al*., 2008] indicates that the two records are only coherent at ~41 and ~23 kyr

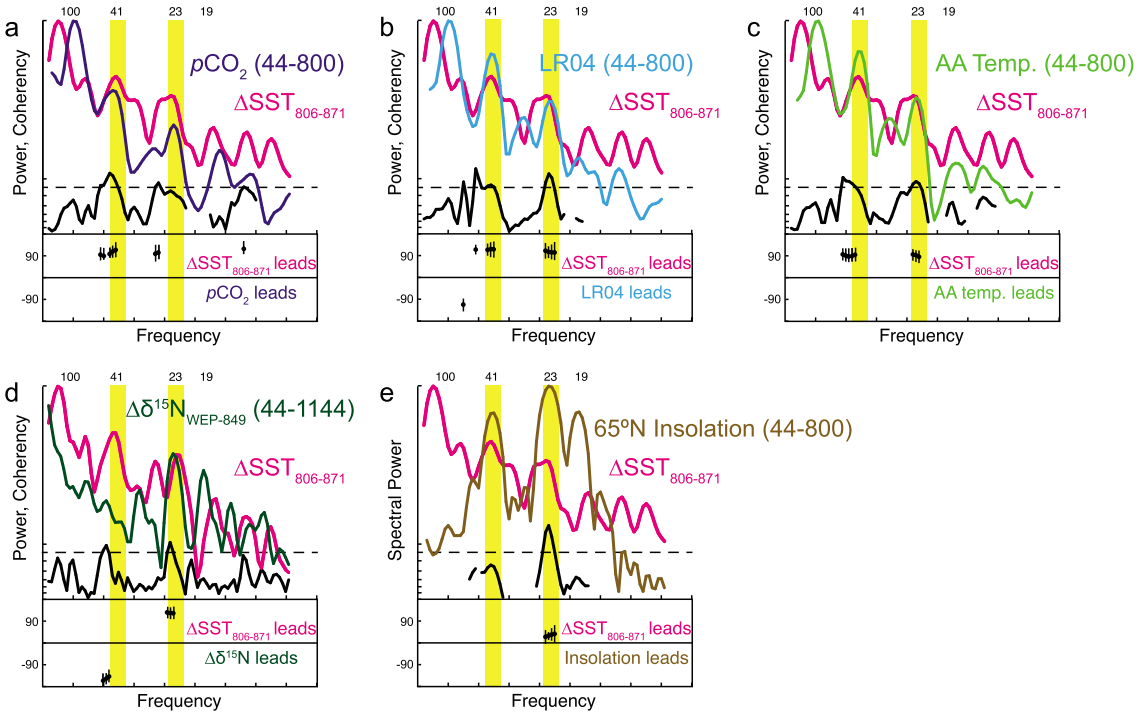

Figure 4. Spectral power, coherence, and phase of $\Delta SST_{806–871}$ (no filter, but resampled at 1 kyr intervals) and (a) pCO_2 [*Lüthi et al.*, 2008], (b) benthic $\delta^{18}O$ [*Lisiecki and Raymo*, 2005], (c) EDC3 Antarctic temperature [*Jouzel et al.*, 2007], (d) $\Delta\delta^{15}N$ (western equatorial Pacific Site 849) [*Rafter and Charles*, 2012], and (e) Northern Hemisphere insolation [*Laskar et al.*, 2004]. All analyses for the period 44–800 ka except Figure 4d.

periodicity; pCO_2 changes lag those in $\Delta SST_{806-871}$ (Figure 4a). This indicates that pCO_2 is not the driving force of variations in $\Delta SST_{806-871}$ and that other forces must be examined.

Coriolis forces and Ekman divergence drive upwelling along the equator; in the modern western equatorial Pacific, the thermocline is below the Ekman layer and therefore upwelled water is relatively warm and does not cool the surface. While greenhouse gases may be the primary driver of broad glacial-interglacial cycles in tropical SSTs in general [*Lea et al.*, 2000; *Lea*, 2004; *Dyez and Ravelo*, 2013], the fact that on-equator cooling exceeded off-equatorial cooling (negative $\Delta SST_{806-871}$) at numerous times throughout the last 1.4 Myr could represent a number of possible factors: (1) stronger wind-driven equatorial upwelling, (2) change in the depth (or tilt) of the thermocline, and/or (3) cooler subsurface source water for equatorial upwelling.

We first consider that stronger tropical surface winds drove greater surface divergence in western Pacific upwelling along the equator, the theoretical point of maximum divergence. If so, we would expect to see coherent and in-phase relationships between proxy records of wind-driven upwelling and $\Delta SST_{806-871}$; unfortunately, no direct records of paleowind strength yet exist for Site 871 or 806. However, variations in eolian grain size and accompanying radiolarian-based indicators of upwelling in the central Pacific [*Chuey et al.*, 1987; *Pisias and Rea*, 1988] are not coherent with variations in $\Delta SST_{806-871}$, suggesting that variability in equatorial winds probably do not explain $\Delta SST_{806-871}$. Because tropical trade wind strength may be affected by remote changes at high latitudes and the pole-to-equator temperature gradients, we also quantified the relationship between $\Delta SST_{806-871}$ and two indicators of high-latitude climate: global ice volume [*Lisiecki and Raymo*, 2005], and Antarctic temperature [*Jouzel et al.*, 2007]. In both cases (Figures 4b and 4c), we found that variations in $\Delta SST_{806-871}$ are coherent, but lead variations in high-latitude conditions, again suggesting that changes in $\Delta SST_{806-871}$ are not forced by atmospheric winds responding to high-latitude climate changes. Wind-driven upwelling and paleoproductivity have been linked to stronger winds in the central and eastern equatorial Pacific [e.g., *Murray et al.*, 1993; *Paytan et al.*, 1996]. One of the longest available paleoproductivity proxy records utilizes the equatorial west-east difference in sedimentary $\delta^{15}N$ [*Rafter and Charles*, 2012]; this record varies coherently, but not in phase with variations in $\Delta SST_{806-871}$ (Figure 4d), once again indicating that wind-driven upwelling is not the main driving force for $\Delta SST_{806-871}$.

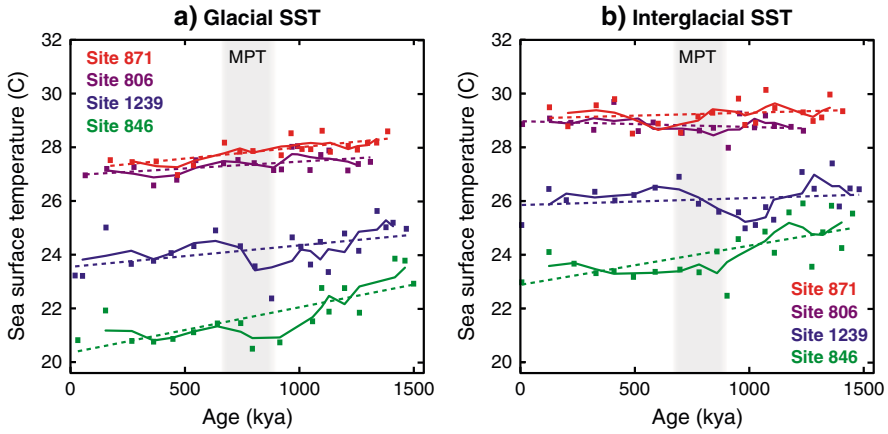

Figure 5. Progression of tropical SST for (a) glacials and (b) interglacials defined by average SST exceeding 1σ standard deviation. Linear fit (dashed line) and three-point moving average (solid line) superimposed.

The second mechanism (a shallower glacial western Pacific thermocline) is an even less likely scenario. Both proxy and numerical model evidence suggest that the western Pacific thermocline was deeper at the Last Glacial Maximum, consistent with stronger Walker circulation [*Andreasen and Ravelo*, 1997; *DiNezio et al.*, 2011]; δ^{18}O evidence also shows that eastern Pacific thermocline depth adjustments occur at 100 kyr cycles [*Cannariato and Ravelo*, 1997]. Although more work is required to reconstruct thermocline depths in the western Pacific, existing evidence contradicts the idea that a shallow glacial thermocline in the west Pacific cooled equatorial SST more than off equatorial SST.

The last of the potential mechanisms—cooler thermocline source water for equatorial upwelling—involves the influence of extratropical conditions on subsurface thermocline temperatures, where equatorial upwelling waters are sourced [e.g., *Holland and Bitz*, 2003; *Fedorov et al.*, 2004] and seems the most promising. *Philander and Fedorov* [2003] proposed that extratropical surface water temperature, controlled by solar forcing, would affect the steepness and temperature of the thermocline, which impacts subsurface source waters in equatorial upwelling regions. We find that $\Delta SST_{806-871}$ is coherent and in phase with Northern Hemisphere summer insolation (but not local insolation) in the precession bandwidth (Figure 4e), which may be related to seasonal changes in the formation of such source water [*Talley*, 1997]. This finding is consistent with theories that the seasonal distribution of extratropical insolation affects tropical SST patterns. Variations in $\Delta SST_{806-871}$ are most likely a result of solar-forced changes in the temperature of thermocline waters, which upwelled in the equatorial Pacific.

3.3. The Zonal Tropical Pacific SST Gradient

Since pCO_2 is thought to be an unlikely candidate for the main driver of the MPT [*Hönisch et al.*, 2009; *Sosdian and Rosenthal*, 2009], ocean dynamics may have played a role in this climate transition. While the western Pacific maintained an average of ~29°C over the past 1.4 Myr, the eastern Pacific average SST cooled from ~24.5°C to ~22.5°C between 1.4 and 0.9 Ma, resulting in a strengthened tropical Pacific zonal gradient (Figures 2 and 5) and Walker circulation that enhanced upwelling or shoaled the eastern Pacific thermocline [e.g., *McClymont and Rosell-Melé*, 2005; *Medina-Elizalde and Lea*, 2005; *Etourneau et al.*, 2010]. Average cold tongue SST then stabilized after the so-called "900 ka event" and did not cool further in the late Pleistocene [*McClymont et al.*, 2013]. The gradual cooling of the cold tongue thus represented the final step in the evolution of the tropical Pacific SST distribution, rather than an earlier date of ~2.0 Ma as previously suggested [*Ravelo et al.*, 2004; *Etourneau et al.*, 2010] and may have preconditioned the Earth system for glacial cooling and ice sheet expansion associated with the MPT [*Brierley and Fedorov*, 2010; *McClymont et al.*, 2013].

Linear regressions of average glacial temperature minima (Figure 5a, dashed lines) at sites from across the tropical Pacific show eastern Pacific SST cooling from 1.5 Ma to present with the cold tongue (Site 846) cooling at a faster rate than other tropical records [*Herbert et al.*, 2010]. The linear regressions of interglacial maxima from warm pool locations (Figure 5b, dashed lines) illustrate, by contrast, the negative feedbacks in the radiative heat budget, atmosphere, or ocean dynamics which work to maintain interglacial warm pool SST within a relatively small range [*Clement et al.*, 1996; *de Garidel-Thoron et al.*, 2005]. Moving

three-point mean curves of peak SST (Figure 5, solid lines) reveal that at the onset of the MPT, the equatorial gradient between the center and margin of the cold tongue (Sites 846 and 1239, respectively) strengthened in both peak glacial and interglacial intervals and then remained roughly constant after ~900 ka. The zonal SST gradient across the Pacific ($\Delta SST_{West\text{-}East}$), defined by subtracting the SST of eastern Site 846 from the average SST of western Sites 871 and 806, also strengthened during the period 1.4–0.9 Ma, both during peak interglacials and glacials (Figure 2d). Thus, the moving mean trace of peak warm pool SST (Figure 5) supports the notion that stronger zonal and meridional tropical Pacific gradients after the MPT onset may have helped to stabilize larger late Pleistocene ice sheets, just as earlier tropical cooling (starting ~4–5 Ma) may have initiated Northern Hemisphere glaciation [*Huybers and Molnar*, 2007; *Brierley and Fedorov*, 2010].

4. Summary

The SST record from ODP Site 806 [*Medina-Elizalde and Lea*, 2005] represents glacial-interglacial SST at the equator but does not quantify the temperature of off equatorial locations; a new high-resolution SST record from off-equator Site 871 (western Pacific warm pool) is presented to evaluate proposed climate forcing mechanisms. Although one forcing agent of tropical SST change is pCO_2, secondary processes involving ocean-atmosphere dynamics also play a role in modulating SST at the equator on orbital timescales and can be monitored by quantifying variation in the SST difference between equatorial Site 806 and off-equatorial Site 871, or $\Delta SST_{806-871}$. Extratropical solar forcing of changes in subsurface thermocline conditions, which affect the temperature of upwelling water at the equator, appears to influence $\Delta SST_{806-871}$.

Using a combination of Pleistocene SST records to reconstruct the zonal Pacific SST gradients, we also show that $\Delta SST_{West\text{-}East}$ increased, both during glacials and interglacials, through the MPT, and then largely stabilized after ~900 ka. Assuming Walker Circulation is tied to the $\Delta SST_{West\text{-}East}$, larger ice sheets and the strong 100 kyr cycle of climate change developed hand in hand with enhanced Walker Circulation.

Acknowledgments

New Mg/Ca and benthic $\delta^{18}O$ data and SST estimates will be uploaded to the National Climate Data Center (NCDC). The Schlanger Fellowship (Consortium for Ocean Leadership) and National Science Foundation grant OCE-0902047 supported this research. The Integrated Ocean Drilling Program provided samples.

Peter Strutton thanks two anonymous reviewers for their assistance in evaluating this paper.

References

Andreasen, D. H., and A. C. Ravelo (1997), Tropical Pacific Ocean thermocline depth reconstructions for the last glacial maximum, *Paleoceanography*, *12*(3), 395–413, doi:10.1029/97PA00822.

Bickert, T., W. H. Berger, S. Burke, H. Schmidt, and G. Wefer (1993), Late Quaternary stable isotope record of benthic foraminifers: Sites 805 and 806, Ontong Java Plateau, in *Proceedings of the Ocean Drilling Program, Scientific Results*, vol. 130, edited by W. H. Berger, L. W. Kroenke, and L. A. Mayer, chap. 24, pp. 411–420, College Station, Tex., doi:10.2973/odp.proc.sr.130.025.

Boyle, E. A., and L. D. Keigwin (1985), Comparison of Atlantic and Pacific paleochemical records for the last 215,000 years: Changes in deep ocean circulation and chemical inventories, *Earth Planet. Sci. Lett.*, *76*(1–2), 135–150, doi:10.1016/0012-821X(85)90154-2.

Brierley, C. M., and A. V. Fedorov (2010), Relative importance of meridional and zonal sea surface temperature gradients for the onset of the ice ages and Pliocene-Pleistocene climate evolution, *Paleoceanography*, *25*, PA2214, doi:10.1029/2009PA001809.

Brierley, C. M., A. V. Fedorov, Z. Liu, T. D. Herbert, K. T. Lawrence, and J. P. LaRiviere (2009), Greatly expanded tropical warm pool and weakened Hadley circulation in the early Pliocene, *Science*, *323*(5922), 1714–1718, doi:10.1126/science.1167625.

Cane, M. A. (1998), A role for the tropical Pacific, *Science*, *282*(5386), 59–61, doi:10.1126/science.282.5386.59.

Cannariato, K. G., and A. C. Ravelo (1997), Pliocene-Pleistocene evolution of eastern tropical Pacific surface water circulation and thermocline depth, *Paleoceanography*, *12*, 805–820, doi:10.1029/97PA02514.

Chuey, J. M., D. K. Rea, and N. G. Pisias (1987), Late Pleistocene paleoclimatology of the central equatorial Pacific: A quantitative record of eolian and carbonate deposition, *Quat. Res.*, *28*(3), 323–339, doi:10.1016/0033-5894(87)90001-9.

Clement, A. C., R. Seager, M. A. Cane, and S. Zebiak (1996), An ocean dynamical thermostat, *J. Clim.*, *9*(9), 2190–2196, doi:10.1175/1520-0442(1996)009<2190:AODT>2.0.CO;2.

de Garidel-Thoron, T., Y. Rosenthal, F. Bassinot, and L. Beaufort (2005), Stable sea surface temperatures in the western Pacific warm pool over the past 1.75 million years, *Nature*, *433*(7023), 294–298, doi:10.1038/nature03189.

Dekens, P. S., A. C. Ravelo, and M. D. Mccarthy (2007), Warm upwelling regions in the Pliocene warm period, *Paleoceanography*, *22*, PA3211, doi:10.1029/2006PA001394.

DiNezio, P. N., A. C. Clement, G. A. Vecchi, B. Soden, A. J. Broccoli, B. L. Otto-Bliesner, and P. Braconnot (2011), The response of the Walker circulation to Last Glacial Maximum forcing: Implications for detection in proxies, *Paleoceanography*, *26*, PA3217, doi:10.1029/2010PA002083.

Dyez, K., and A. C. Ravelo (2013), Late Pleistocene tropical Pacific temperature sensitivity to radiative greenhouse gas forcing, *Geology*, *41*(1), 23–26, doi:10.1130/G33425.1.

Etourneau, J., R. R. Schneider, T. Blanz, and P. Martinez (2010), Intensification of the Walker and Hadley atmospheric circulations during the Pliocene-Pleistocene climate transition, *Earth Planet. Sci. Lett.*, *297*, 103–110, doi:10.1016/j.epsl.2010.06.010.

Farrell, J. W., and W. L. Prell (1989), Climatic change and $CaCO_3$ preservation: An 800,000 year bathymetric reconstruction from the central equatorial Pacific Ocean, *Paleoceanography*, *4*(4), 447–466, doi:10.1029/PA004i004p00447.

Farrell, J. W., and W. L. Prell (1991), Pacific $CaCO_3$ preservation and $\delta^{18}O$ since 4 Ma: Paleoceanographic and paleoclimatic implications, *Paleoceanography*, *6*(4), 485–498, doi:10.1029/91PA00877.

Fedorov, A. V., R. C. Pacanowski, S. G. Philander, and G. Boccaletti (2004), The effect of salinity on the wind-driven circulation and the thermal structure of the upper ocean, *J. Phys. Oceanogr.*, *34*(9), 1949–1966, doi:10.1175/1520-0485(2004)034<1949:TEOSOT>2.0.CO;2.

Herbert, T. D., L. C. Peterson, K. T. Lawrence, and Z. Liu (2010), Tropical ocean temperatures over the past 3.5 million years, *Science*, *328*, 1530–1534, doi:10.1126/science.1185435.

Holland, M. M., and C. M. Bitz (2003), Polar amplification of climate change in coupled models, *Clim. Dyn.*, *21*(3–4), 221–232, doi:10.1007/s00382-003-0332-6.
Hönisch, B., N. G. Hemming, D. Archer, M. Siddall, and J. F. McManus (2009), Atmospheric carbon dioxide concentration across the mid-Pleistocene transition, *Science*, *324*(5934), 1551, doi:10.1126/science.1171477.
Huybers, P., and P. Molnar (2007), Tropical cooling and the onset of North American glaciation, *Clim. Past*, *3*(3), 549–557, doi:10.5194/cp-3-549-2007.
Jouzel, J., et al. (2007), Orbital and millennial Antarctic climate variability over the past 800,000 years, *Science*, *317*(5839), 793–796, doi:10.1126/science.1141038.
Karas, C., D. Nürnberg, A. K. Gupta, R. Tiedemann, K. Mohan, and T. Bickert (2009), Mid-Pliocene climate change amplified by a switch in Indonesian subsurface throughflow, *Nat. Geosci.*, *2*(6), 434–438, doi:10.1038/ngeo520.
Knutson, T., and S. Manabe (1995), Time-mean response over the tropical Pacific to increased CO_2 in a coupled ocean–atmosphere model, *J. Climate*, *8*(9), 2181–2199, doi:10.1175/1520-0442(1995)008<2181:TMROTT>2.0.CO;2.
Koutavas, A., and J. Lynch-Stieglitz (2005), Variability of the Marine ITCZ over the eastern Pacific during the past 30,000 years: Regional perspective and global context, in *The Hadley Circulation: Present, Past and Future*, edited by H. F. Diaz and R. S. Bradley, pp. 347–369, Springer Academic Publishers, Boston, Mass.
Koutavas, A., J. Lynch-Stieglitz, T. Marchitto, and J. Sachs (2002), El Nino-like pattern in ice age tropical Pacific sea surface temperature, *Science*, *297*(5579), 226–230, doi:10.1126/science.1072376.
Laskar, J., P. Robutel, F. Joutel, M. Gastineau, A. C. M. Correia, and B. Levrard (2004), A long-term numerical solution for the insolation quantities of the Earth, *Astron. Astrophys.*, *428*(1), 261–285, doi:10.1051/0004-6361:20041335.
Lea, D. W. (2004), The 100 000-yr cycle in tropical SST, greenhouse forcing, and climate sensitivity, *J. Clim.*, *17*(11), 2170–2179, doi:10.1175/1520-0442(2004)017<2170:TYCITS>.
Lea, D. W., D. K. Pak, and H. J. Spero (2000), Climate impact of late Quaternary equatorial Pacific sea surface temperature variations, *Science*, *289*(5485), 1719–1724, doi:10.1126/science.289.5485.1719.
Lea, D. W., D. K. Pak, C. L. Belanger, H. J. Spero, M. A. Hall, and N. J. Shackleton (2006), Paleoclimate history of Galapagos surface waters over the last 135,000 yr, *Quat. Sci. Rev.*, *25*(11–12), 1152–1167, doi:10.1016/j.quascirev.2005.11.010.
Lisiecki, L. E., and M. E. Raymo (2005), A Pliocene-Pleistocene stack of 57 globally distributed benthic δ^{18}O records, *Paleoceanography*, *20*, PA1003, doi:10.1029/2004PA001071.
Liu, Z., and T. D. Herbert (2004), High-latitude influence on the eastern equatorial Pacific climate in the early Pleistocene epoch, *Nature*, *427*(6976), 720–723, doi:10.1038/nature02338.
Liu, Z., S. Vavrus, F. He, N. Wen, and Y. Zhong (2005), Rethinking tropical ocean response to global warming: The enhanced equatorial warming, *J. Clim.*, *18*(22), 4684–4700, doi:10.1175/JCLI3579.1.
Locarnini, R. A., et al. (2013), World ocean atlas 2013, in *NOAA Atlas NESDIS 73*, Temperature, vol. 1, edited by S. Levitus and A. Mishonov, p. 40, U.S. Government Printing Office, Washington, D. C.
Lüthi, D., et al. (2008), High-resolution carbon dioxide concentration record 650,000–800,000 years before present, *Nature*, *453*(7193), 379–382, doi:10.1038/nature06949.
Mashiotta, T., D. W. Lea, and H. J. Spero (1999), Glacial-interglacial changes in subantarctic sea surface temperature and δ^{18}O-water using foraminiferal Mg, *Earth Planet. Sci. Lett.*, *170*(4), 417–432, doi:10.1016/S0012-821X(99)00116-8.
McClymont, E. L., and A. Rosell-Melé (2005), Links between the onset of modern Walker circulation and the mid-Pleistocene climate transition, *Geology*, *33*(5), 389, doi:10.1130/G21292.1.
McClymont, E. L., S. M. Sosdian, A. Rosell-Melé, and Y. Rosenthal (2013), Pleistocene sea-surface temperature evolution: Early cooling, delayed glacial intensification, and implications for the mid-Pleistocene, *Earth Sci. Rev.*, *123*, 173–193, doi:10.1016/j.earscirev.2013.04.006.
Medina-Elizalde, M., and D. W. Lea (2005), The mid-Pleistocene transition in the Tropical Pacific, *Science*, *310*(5750), 1009–1012, doi:10.1126/science.1115933.
Murray, R. W., M. Leinen, and A. R. Isern (1993), Biogenic flux of Al to sediment in the central equatorial Pacific Ocean: Evidence for increased productivity during glacial periods, *Paleoceanography*, *8*(5), 651–670, doi:10.1029/93PA02195.
Palliard, D., L. Labeyrie, and P. Yiou (1996), Macintosh program performs time-series analysis, *Eos Trans. AGU*, doi:10.1029/96EO00259.
Paytan, A., M. Kastner, and F. P. Chavez (1996), Glacial to interglacial fluctuations in productivity in the equatorial Pacific as indicated by marine barite, *Science*, *274*(5291), 1355–1357, doi:10.1126/science.274.5291.1355.
Philander, S. G., and A. V. Fedorov (2003), Role of tropics in changing the response to Milankovich forcing some three million years ago, *Paleoceanography*, *18*(2), 1045, doi:10.1029/2002PA000837.
Pisias, N. G., and D. K. Rea (1988), Late Pleistocene paleoclimatology of the central equatorial Pacific: Sea surface response to the southeast trade winds, *Paleoceanography*, *3*(1), 21–37, doi:10.1029/PA003i001p00021.
Rafter, P. A., and C. D. Charles (2012), Pleistocene equatorial Pacific dynamics inferred from the zonal asymmetry in sedimentary nitrogen isotopes, *Paleoceanography*, *27*, PA3102, doi:10.1029/2012PA002367.
Ramanathan, V., and W. Collins (1991), Thermodynamic regulation of ocean warming by cirrus clouds deduced from observations of the 1987 El Niño, *Nature*, *351*(6321), 27–32, doi:10.1038/351027a0.
Ravelo, A. C., D. H. Andreasen, M. Lyle, A. Olivarez Lyle, and M. W. Wara (2004), Regional climate shifts caused by gradual global cooling in the Pliocene epoch, *Nature*, *429*(6989), 263–267, doi:10.1038/nature02567.
Schlitzer, R. (2014), Ocean data view, 4th ed. [Available at http://www.odv.awi.de.]
Shipboard Scientific Party (1993), Site 871, in *Proceedings of the Ocean Drilling Program, Initial Reports*, vol. 144, edited by P. I. Silva, J. Haggerty, and R. Rack, pp. 105–144, Ocean Drilling Program, College Station, Tex.
Sosdian, S., and Y. Rosenthal (2009), Deep-sea temperature and ice volume changes across the Pliocene-Pleistocene climate transitions, *Science*, *325*(5938), 306–310.
Sun, D. Z. (2003), A possible effect of an increase in the warm-pool SST on the magnitude of El Niño warming, *J. Clim.*, *16*(2), 185–205, doi:10.1175/1520-0442(2003)016<0185:APEOAI>2.0.CO;2.
Talley, L. D. (1997), North Pacific intermediate water transports in the mixed water region, *J. Phys. Oceanogr.*, *27*, 1795–1803, doi:10.1175/1520-0485(1997)027<1795:NPIWTI>2.0.CO;2.
Thompson, P. R., and T. Saito (1974), Pacific Pleistocene sediments: Planktonic foraminifera dissolution cycles and geochronology, *Geology*, *2*(7), 333, doi:10.1130/0091-7613(1974)2<333:PPSPFD>2.0.CO;2.
Wallace, J. (1992), Effect of deep convection on the regulation of tropical SST, *Nature*, *377*, 230–231, doi:10.1038/357230a0.
Wara, M. W., A. C. Ravelo, and M. L. Delaney (2005), Permanent El Niño-like conditions during the Pliocene warm period, *Science*, *309*(5735), 758–761, doi:10.1126/science.1112596.

Auxiliary Material for

Dynamical changes in the tropical Pacific warm pool and zonal gradient during the Pleistocene

Kelsey A. Dyez[1]*, A. Christina Ravelo[2]

[1]*Earth and Planetary Sciences, University of California Santa Cruz, Santa Cruz, California, USA*
**currently at: Lamont-Doherty Earth Observatory, Columbia University, Palisades, New York, USA*

[2]*Ocean Sciences, University of California Santa Cruz, Santa Cruz, California, USA*

Geophysical Research Letters

The Supplementary Table contains peak glacial and interglacial intervals based on the LR04 benthic $\delta^{18}O$ stack, calculated as described in the main body of the manuscript.

1.1 Column "Marine Isotope Stage", Marine Isotope Stage number
1.2 Column "Age (kyr) Start", Age (in kiloyears) at which peak glacial or interglacial interval started
1.3 Column "Age (kyr) End", Age (in kiloyears) at which peak glacial or interglacial interval ended

Table SI. Peak glacial and interglacial intervals.

Marine Isotope Stage	Age (kyr) Start	Age (kyr) End
1	11	0
2	25	17
5	127	116
6	157	135
7	242	199
8	277	250
9	334	315
10	363	340
11	417	397
12	448	429
13	503	484
14	556	536
15	616	572
16	640	626
17	704	690
18	750	716
19	788	774
20	840	794
21	860	850
22	876	872
23	914	908
24	926	918
25	956	948
26	966	962
27	980	978
28	1008	986
29	1024	1022
30	1044	1034
31	1074	1068
32	1099	1097
33	1112	1106
34	1128	1122
35	1168	1160
36	1208	1198
37	1240	1230
38	1254	1248
39	1282	1276
40	1298	1288
41	1318	1310
42	1340	1334
43	1358	1350
44	1378	1368
45	1400	1392
46	1414	1410
47	1440	1436
48	1464	1454
49	1480	1474
50	1500	1496